
Princeton Plasma Physics Laboratory

PPPL-

PPPL-



Prepared for the U.S. Department of Energy under Contract DE-AC02-09CH11466.

Princeton Plasma Physics Laboratory

Report Disclaimers

Full Legal Disclaimer

This report was prepared as an account of work sponsored by an agency of the United States Government. Neither the United States Government nor any agency thereof, nor any of their employees, nor any of their contractors, subcontractors or their employees, makes any warranty, express or implied, or assumes any legal liability or responsibility for the accuracy, completeness, or any third party's use or the results of such use of any information, apparatus, product, or process disclosed, or represents that its use would not infringe privately owned rights. Reference herein to any specific commercial product, process, or service by trade name, trademark, manufacturer, or otherwise, does not necessarily constitute or imply its endorsement, recommendation, or favoring by the United States Government or any agency thereof or its contractors or subcontractors. The views and opinions of authors expressed herein do not necessarily state or reflect those of the United States Government or any agency thereof.

Trademark Disclaimer

Reference herein to any specific commercial product, process, or service by trade name, trademark, manufacturer, or otherwise, does not necessarily constitute or imply its endorsement, recommendation, or favoring by the United States Government or any agency thereof or its contractors or subcontractors.

PPPL Report Availability

Princeton Plasma Physics Laboratory:

<http://www.pppl.gov/techreports.cfm>

Office of Scientific and Technical Information (OSTI):

<http://www.osti.gov/bridge>

Related Links:

[U.S. Department of Energy](#)

[Office of Scientific and Technical Information](#)

[Fusion Links](#)

Molecular hydrogen density measurements of short-pulse, high-density fueling from a molecular cluster injector

D.P. Lundberg, R. Kaita and R. Majeski

Princeton Plasma Physics Laboratory, Princeton, NJ, 08543 USA

E-mail: dlundberg@pppl.gov

Abstract. A Molecular Cluster Injector (MCI) has been developed to provide short-pulse, high-density fueling for the Lithium Tokamak Experiment (LTX). Using an electron beam fluorescence method, the molecular density profiles produced by the injector are measured with sub-cm spatial resolution. The system, which is cryogenically cooled to promote the formation of molecular clusters, demonstrates a significant increase in molecular density relative to room-temperature supersonic gas injectors. The transient characteristics of short pulses (3-5ms) are measured with $250\mu\text{s}$ temporal resolution, and the jet shock structure is found to evolve significantly on that time scale. Supplemental measurements with a pressure transducer validate the electron beam measurements. The measured density profiles are consistent with supersonic flows suitable for producing substantial populations of molecular clusters. The measured densities and flow-rates are appropriate for high-density fueling of LTX plasmas. The MCI will be used to investigate the physics of molecular cluster fueling of LTX plasmas.

PACS numbers: 52.25.Ya, 34.80.Gs, 28.52.Cx

1. Introduction

Historically, the fueling of fusion experiments has primarily consisted of wall-mounted gas puffers and pellet injectors. Wall-mounted puffers produce a diffuse, undirected flow. This results in poor fueling efficiency, where only 10% or less of the particles penetrate past the plasma edge. Puffers generally have a long guide tube between the valve and plasma edge. This allows gas to trickle into the plasma volume long after the valve is closed, preventing fine temporal control of the fueling rate. Pellet injectors have fueling efficiencies of 50% for low field side injection, and up to 100% for high field side injection [1]. They produce temporally well-defined particle sources, and the size of the pellets can be scaled to match particle inventory requirements for small and large machines. But systems that produce multiple pellets for steady fueling are complex and expensive, making them ill-suited for small experiments.

More recently, as an intermediate fueling source, supersonic gas injectors were developed. These consist of a fast pulse valve and supersonic nozzle on a movable feedthrough, placing them close to the plasma edge. This results in a high density, directed particle source, with fueling efficiencies often in excess of 30% [2, 3]. Because the volume filled with gas is small, the flow shuts off quickly once the valve is closed, allowing the study of transient fueling [4]. However, the gas density falls off quickly away from the nozzle, and the fueling efficiencies obtained lag pellet injection systems by a sizeable margin.

1.1. Fueling with Molecular Clusters

To improve on supersonic gas injection, it has been proposed to cryogenically cool the valve, nozzle, and gas reservoir, promoting the formation of molecular clusters [5]. The goal is to create higher fueling efficiency and deeper “pellet-like” fueling with relatively simple inexpensive equipment. Experiments on HL-2A indicated a substantial improvement in how far neutrals penetrated into plasmas when the supersonic gas injection system was cooled with liquid nitrogen, and suggested that the presence of molecular clusters was the reason [6]. The ionization cross-section of clusters has been shown to be smaller than an equal number of single molecules, suggesting one possible mechanism for deeper penetration [7]. However, the cross-section is only significantly reduced for very large clusters, i.e., at least 10^4 molecules.

For smaller clusters, such as those in [6], the high neutral density in the collimated flow may be the salient parameter. Previous analytic work has proposed that if the total density of gas-phase molecules and clusters at the plasma is high enough, neutrals will penetrate deeper into the plasma than the single-particle mean-free-path, as in a pellet ablation cloud [8]. Cluster formation and molecular density are correlated, so it is difficult to separate the two factors. Regardless of the exact details of the plasma-neutral interaction, by cooling the gas and forming clusters, molecules are focused closer to the jet axis. This maintains a higher neutral density over a longer distance. Thus cluster sources present an opportunity for improving fueling efficiency, while maintaining the fast response and technical simplicity of a supersonic gas injection system.

1.2. Application to the Lithium Tokamak Experiment

A Molecular Cluster Injector (MCI), consisting of a liquid nitrogen-cooled fast solenoid valve and supersonic nozzle, has been developed for the Lithium Tokamak Experiment

(LTX) [9]. The LTX is a small spherical torus designed to have lithium cover 90% of the plasma facing surfaces, which is expected to reduce the influx of recycled neutral particles into the plasma edge and substantially increase external fueling requirements. The LTX will study modifications to the plasma density profile as the externally supplied fueling varies between several cases: gas puffer edge fueling, edge and partial core fueling with supersonic gas injection, and core fueling with the MCI.

The MCI will also be used to study the extreme case of a low-recycling plasma with all externally applied fueling turned off. The MCI will inject a short, high-density pulse with high fueling efficiency to supply a large initial particle inventory in the core. After the fast turn-off time (less than 1 ms) of the MCI, the only remaining particle source is the relatively small flux from the low-recycling walls, and the plasma density will quickly decay. The MCI is necessary because puffers and supersonic gas injectors source too many neutral particles outside of the last closed flux surface, making it difficult to discriminate between the external fueling and the remaining flux from the wall. Furthermore, the higher throughput and core fueling of the MCI will provide a larger initial particle inventory, allowing a longer period of time before the plasma becomes unstable due to a low density. In conjunction with low-recycling walls, the MCI is a tool to provide access to a novel tokamak operating regime, where the density profile is no longer dominated by an edge particle flux.

In the absence of external fueling, the density decay is determined by the effective particle confinement time, τ_p^* , which is related to the particle confinement time τ_p through the recycling coefficient R : $\tau_p^* = \tau_p / (1 - R)$. Under high-recycling conditions, τ_p^* is often too long to measure. For low-recycling conditions (small R), τ_p^* can approach τ_p . For example, on CDX-U, which employed a partial liquid lithium limiter, τ_p^* was measured to be between 2-15 ms, depending on the amount and condition of the lithium coverage [4, 10]. Under very low-recycling conditions with external fueling shut off, the temperature profile is predicted to become flat, eliminating anomalous conductive transport [11, 12]. Under these conditions, energy confinement would be determined by particle confinement, i.e., $\tau_E \sim \tau_p$. The density gradient will relax to minimize ∇n transport. With the ∇T and ∇n drive terms greatly reduced, particle losses should be determined by ion neoclassical transport. With full low-recycling plasma facing components and the high-throughput pulsed fueling provided by the MCI, the LTX will be able to study particle confinement, and with separate energy confinement measurements, test these predictions.

Previous studies on hydrogen cluster formation within supersonic jets were generally concerned with studying the interactions of clusters with lasers [13, 14] and accelerator beams [15]. While robust empirical scaling laws for molecular cluster size and number density were determined, the characteristics of the gas phase molecule population were not of primary interest. Often the gas-phase molecules were actively removed with a series of skimmers and large vacuum pumps. Even previous work on cluster sources for fusion fueling largely concentrated on Raleigh scattering measurements of the cluster size close to the nozzle outlet [6]. However, a liquid nitrogen-cooled hydrogen MCI will only produce a minority cluster population. Given the uncertainty in the neutral penetration mechanism into fusion plasmas, it may be detrimental to discard the gas-phase population in a fueling system. Furthermore, conditions within a few millimeters of the nozzle are irrelevant. It is important to know the neutral density at a location comparable to the plasma location, i.e., tens of centimeters from the nozzle outlet.

In this work we characterize the molecular densities produced by the MCI

to evaluate its appropriateness as a fueling source for LTX. Note that the term “molecular density” is inclusive of the cluster population. The cluster population is not independently measured, as the prior literature on cluster formation with similar hardware is comprehensive [13, 14, 15, 16]. Using an electron beam fluorescence method, molecular density profiles are measured with sub-cm spatial resolution. Full two-dimensional profiles are reconstructed for several operating conditions. The supersonic jets produced with two conical nozzles are compared; a 4.5° Mach 5.5 nozzle is found to produce densities an order of magnitude higher than a 45° Mach 3 nozzle. Cooling the injector to 80 K with liquid nitrogen produces densities a factor of six higher than the room-temperature case. The higher density of the cold jets may provide an improvement in fueling performance relative to the room-temperature case (equivalent to a conventional supersonic gas injector). Note that this is even without considering any microscopic effects from the cluster population, such as a reduction in the effective ionization cross-section.

The MCI produces high-density, collimated flows with molecular densities in excess of 10^{15} cm^{-3} more than 20 cm from the nozzle. These densities are 100-1000 times LTX plasma densities. The transient properties of 3-8 ms pulses, including details of the shock structure, are measured with $250 \mu\text{s}$ resolution, and found to evolve significantly on a millisecond time-scale. The flows are consistent with supersonic jets suitable for substantial cluster formation. A supplementary set of measurements on the 45° nozzle with a pressure transducer are presented, with good quantitative agreement providing validation of the electron beam results. The attenuation of the 250 eV electron beam is measured to estimate whether an MCI fueling pulse can fully absorb LTX electrons. With valve backing pressures over 100 psi (0.69 MPa), 250 eV electrons can be fully absorbed, suggesting access to a high-density fueling regime is possible. The cryogenic MCI provides total fueling rates of $1.5 \cdot 10^{22} - 6 \cdot 10^{22} \text{ H}_2$ molecules/second at backing pressures of 50-250 psi (0.35-1.75 MPa), making it suitable for short-pulse replacement of the LTX particle inventory.

2. Supersonic Jets in Vacuum

The general structure of a free jet expanding into vacuum is well known [17], and is summarized in Figure 1. The gas undergoes an isentropic expansion in the nozzle and into vacuum, forming a supersonic region known as the “zone of silence.” Theoretically, the properties of this region are independent of the ambient pressure. The jet is surrounded by an axial “barrel shock,” and terminates downstream at a shock known as the “Mach disk.” The sizes and locations of the shocks depend on the nozzle shape, Mach number (M_D), and diameter (D_N), as well as the valve backing pressure (P_o), and the ambient vacuum pressure (P_B). For a sonic nozzle, the distance from the nozzle to the Mach disk (X_M) is known to be [18]:

$$X_M = 0.67D_N \left(\frac{P_o}{P_B} \right)^{1/2} \quad (1)$$

The Mach disk and barrel shock diameters also scale as $(P_o/P_B)^{1/2}$. There is no general formula for a supersonic nozzle, as the shape of the expansion is dependent on the nozzle geometry, but the scalings are expected to have the same dependence on the pressure ratio.

The gas cools as it expands in the diverging nozzle section into vacuum, and if the initial temperature is sufficiently low, clusters form via Van der Waals attraction

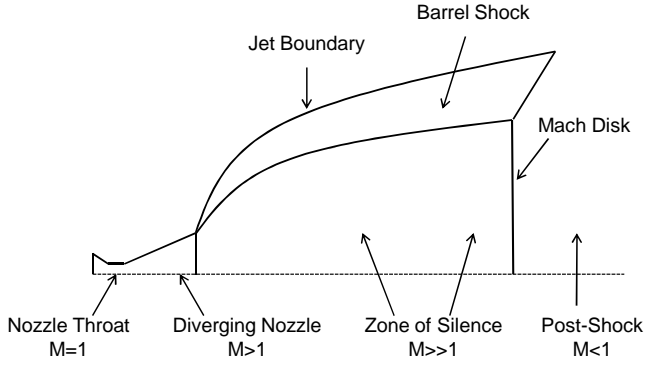


Figure 1. The generic shape of the shock structure for a free jet expanding into vacuum. Gas undergoes an isentropic expansion from the nozzle into vacuum, and forms a supersonic “zone of silence,” until a “Mach disk” is formed downstream. The axial shock boundary is called the “barrel shock.”

as cold molecules collide. Past a certain distance, the density drops below a critical threshold, collisions become rare, and the flow properties remain static as supersonic molecules (and clusters, if they are present) free-stream on ballistic trajectories through the zone of silence and into the plasma target. However, if P_B is high enough, the Mach disk will appear between the nozzle and plasma, and collisions with warm, post-shock molecules will destroy clusters and slow molecules to subsonic speeds [19]. In practice, this means that P_B must be held low by limiting the valve opening time or through extensive pumping. To determine the extent of these concerns for a fueling system, we characterize the jet as it expands into a modest finite volume with limited pumping. These operating conditions are comparable to when the MCI is mounted on the LTX.

3. The Molecular Cluster Injector

A Series 99 Parker fast solenoid valve (Parker Valve Corp. Fairfield NJ, USA) is surrounded by a tight-fitting copper cooling jacket, see Figure 2. Liquid nitrogen flows through 3.2 mm copper tubing brazed to the exterior of the jacket. The valve itself contains a converging section, and a diverging conical nozzle is attached to the valve face with an indium wire seal. While contoured Laval nozzles are known to produce collimated supersonic gas flows, they must be designed for steady-state operation at a single P_B . This system is pulsed, with P_B typically spanning 10^{-7} - 10^{-2} torr. Additionally, conical nozzles have been measured to be superior for the formation of molecular clusters [13]. For these reasons, as well as ease of fabrication, conical nozzles were used. One such nozzle, with a 45° half-angle, was available pre-cut into the valve face from the manufacturer, with a 0.51 mm throat, 1.02 mm outlet diameter, and a design Mach number $M_D = 3$. An additional nozzle with a 4.5° half-angle was fabricated from type 316 stainless steel. This design has $M_D = 5.5$, with 0.51 mm throat and 3.2 mm outlet diameters.

The valve is mounted on a thin-wall cryogenic vacuum feed-through. VCR fittings form the vacuum-side connections to the valve H_2 line and cooling jacket liquid nitrogen lines. Apiezon N (M&I Materials Ltd. Manchester, UK) grease is used

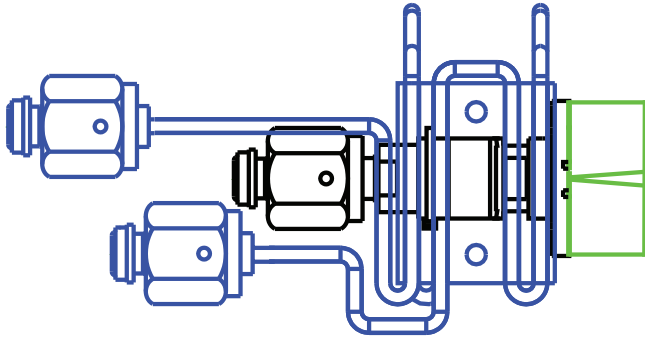


Figure 2. The fast solenoid valve (black) is surrounded by a copper cooling block with 3.2 mm copper liquid-nitrogen lines (blue). An indium wire seal in the valve face o-ring groove mates a supersonic nozzle (green) to the valve. VCR fittings are used for cryogenic vacuum seals.

to maintain good thermal conductivity between the valve body, cooling jacket, and nozzle at cryogenic temperatures. Temperatures of 80 K are routinely achieved, and are monitored by a platinum RTD sensor potted in the cooling block with Apiezon N. The valve is rated for use up to 1250 psi (8.62 MPa) and operates reliably at cryogenic temperatures, although it does have a measurable H_2 leak rate below about 100 K. Typical cryogenic operation consists of P_o from 50-250 psi (0.35-1.75 MPa) and 3-8 ms pulses, though opening times as short as 500 μs are possible.

4. Electron Beam Measurements of Molecular Density Profiles

Electron-induced fluorescence has long been used for imaging of gas jets. However, for quantitative measurements, prior methods primarily used high-energy electron sources to keep the mean-free-path of the electrons long relative to the gas jet [20]. While this means that the electron beam (“e-beam”) can be treated as uniform across the entire gas jet, the electron densities are low, and long exposures in steady-state conditions are required to collect sufficient light. However, the MCI is a pulsed system, and the transient properties of the flow are important. A low-energy e-beam source, 250V with 10 mA of electron current, provides enough light through an H_α filter for a Phantom Miro 2 fast camera (Vision Research, Wayne, NJ, USA) to record single frames as short as 250 μs with low-noise and high repeatability. This allows the study of transient features, such as evolving shock structures.

4.1. Apparatus and Calibration

The apparatus used is the same as described in reference [22] see Figure 3. The e-beam is oriented perpendicular to the jet axis, providing a transverse profile at a single distance, x , from the nozzle. To construct two-dimensional density profiles, x was varied in 1 cm steps from 4-22 cm. The individual profiles were combined and smoothed with a 2-D interpolation.

Electrons at 250 eV have a mean-free-path longer than a 10 cm jet for molecular densities less than about $1 \cdot 10^{15} \text{ cm}^{-3}$ [21]. For densities below this threshold, the e-beam approximately maintains its initial energy and density, and a simple absolute calibration of the emission is sufficient. The chamber (of known volume and

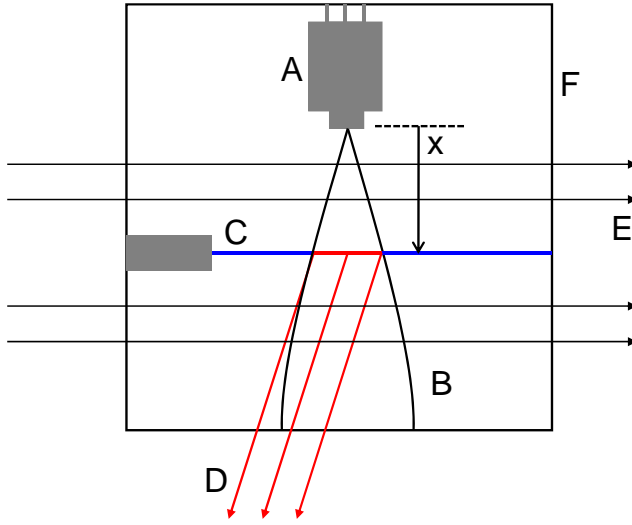


Figure 3. The solenoid valve and nozzle (A), produce a collimated gas jet (B). The e-beam (C), a distance x away from the nozzle, collides with the jet and produces emission (D) that is viewed through an H_{α} filter by a fast camera. The e-beam is confined by a 75 G magnetic field (E). The experiment is contained in a 175 liter vacuum tank (F)

temperature) is filled with H_2 , and the pressure is measured with a type 626 Baratron (MKS Instruments, Andover, MA, USA) to determine the molecular density. The e-beam is passed through the chamber, and the emission per H_2 molecule can then be determined for a given set of camera parameters. Images of the fluorescence captured with the same camera parameters can then be converted into absolute molecular density profiles. This method can be used for room-temperature and cryogenic jets with P_o up to about 50 psi (0.35 MPa).

For line-integrated molecular densities much higher than $1 \cdot 10^{16} \text{ cm}^{-2}$, the beam properties are substantially altered by collisions with the jet. As previously described [22], the H_2 density profile can be determined even when the jet density is high enough to cause severe e-beam attenuation. Cryogenic jets with P_o above 50 psi (0.35 MPa) require the use of this e-beam attenuation method. For intermediate jet densities, the attenuation method and the absolute calibration method can be compared, and generally agree to within 10-25%. This is comparable to the systematic error in the attenuation method.

4.2. Comparison of Room-Temperature and Cryogenic Jet

The reconstructed density profiles in Figure 4 are of 50 psi (0.35 MPa) pulses from both the room-temperature (295 K, top image) and cryogenic (80 K, bottom image) injector with the 4.5° nozzle. To illustrate the stark difference in the two cases, we have selected the last 1 ms of a 4 ms pulse, after the background pressure has risen significantly. The room-temperature injector creates a relatively well-collimated flow, but 4 cm from the nozzle the density is less than $5 \cdot 10^{15} \text{ cm}^{-3}$. It drops below the measurement sensitivity of $\sim 1 \cdot 10^{15} \text{ cm}^{-3}$ in less than 10 cm. No shock structure

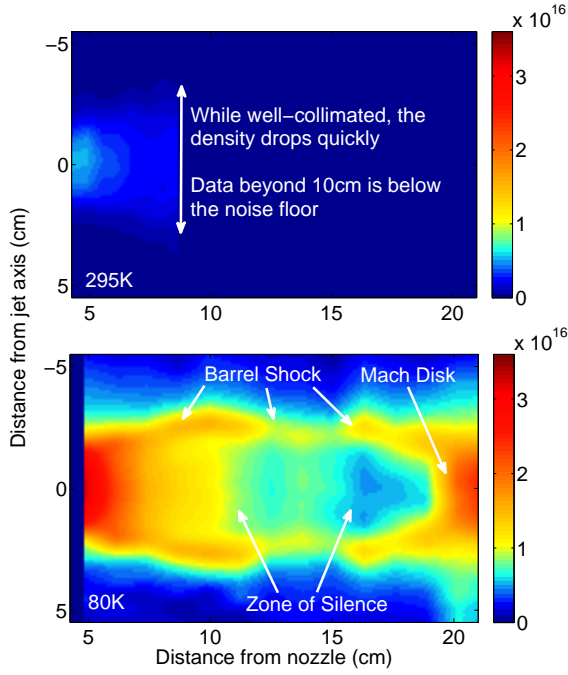


Figure 4. The room-temperature valve (top) produces a low-density jet without measurable shock structures, while the cryogenic jet (bottom) creates shock structures identifiable as those pictured in Figure 1. Both cases use $P_o = 50$ psi (0.35 MPa). The density units are cm^{-3} .

is visible. While the expected shock size scaling of $(P_o/P_B)^{1/2}$ implies a finite shock for any value of (P_o/P_B) , it has been previously found that for a fixed P_o/P_B with both pressures decreasing, the shock width decreases until it finally vanishes [17]. This implies that the 295 K injector produces modest densities and ill-defined jet boundaries that allow significant intrusion of background gas into the jet interior. This allows collisions to scatter supersonic molecules and degrade the collimation. In contrast, the 50 psi (0.35 MPa) injector cooled to 80 K produces molecular densities over $3 \cdot 10^{16} \text{ cm}^{-3}$ at 4 cm from the nozzle, and above $4 \cdot 10^{15} \text{ cm}^{-3}$ out to 20 cm from the nozzle. The shock structures in the 80 K injector case are clearly identifiable as those outlined in Figure 1, with an extended zone of silence. The Mach disk becomes visible at 4 ms due to the rapid increase of P_B .

4.3. Fast Time-Scale Evolution of the Molecular Density

To examine the transient nature of the shock structure, an entire 4 ms, 100 psi (0.69 MPa) pulse was reconstructed (see Figure 5). The frames are 1 ms exposures, staggered by 1 ms. In the first frame, the density gradient along the axis is flatter, suggesting that the flow is still forming into a stable supersonic jet. This suggests using opening times of at least 2 ms to ensure quiescent flows suitable for cluster

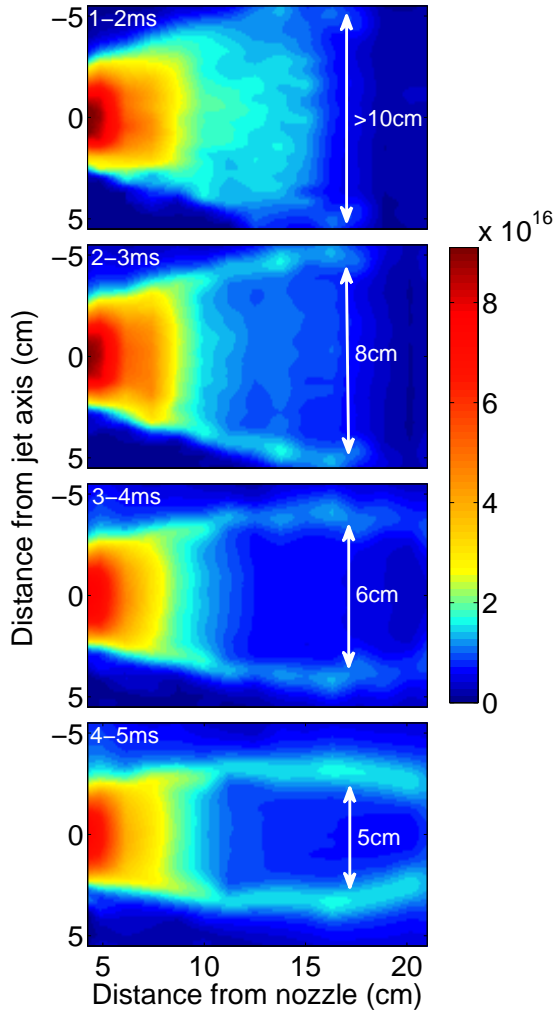


Figure 5. The 100 psi (0.69 MPa), cryogenic jet. Each frame is 1 ms of a 4 ms pulse. After taking 1 ms to settle, the density (units of cm^{-3}) in the zone of silence is effectively constant. The barrel shock diameter narrows substantially in 4 ms.

formation. The density in the zone of silence is nearly identical in the three later frames, except for a 10% drop corresponding to the decline of P_o over the length of the pulse. For example, 10 cm from the nozzle, the central density in frames 2-4 is $1.51 \cdot 10^{16} \text{ cm}^{-3}$, $1.33 \cdot 10^{16} \text{ cm}^{-3}$, and $1.30 \cdot 10^{16} \text{ cm}^{-3}$. The jet has an elongated shock structure, consistent with a directed, high Mach number flow. The zone of silence is visible across the entire view (more than 60 nozzle diameters long). The shock structure evolves significantly over the pulse length. The barrel shock diameter shrinks from more than 10 cm down to 5 cm, reflecting the substantial increase in P_B .

To further understand the evolution of the shock structure, the jet diameter was measured as a function of P_o and the time elapsed from the valve opening, t (see

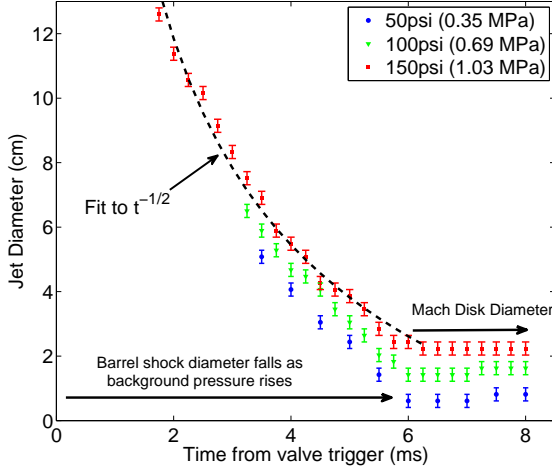


Figure 6. The jet diameter measured 22 cm from the nozzle. The diameter initially shrinks as the barrel shock shrinks as $t^{-1/2}$. After 6 ms, the Mach disk is in view, and the diameter stays roughly constant from 6-8 ms. This Mach disk diameter is linearly dependent on the backing pressure.

Figure 6). Valve openings of 8 ms were used, with P_o of 50, 100, and 150 psi (0.35, 0.69, and 1.03 MPa). Because the H_α filter limits the view to a ~ 10 cm viewing angle, the 150 psi (1.03 MPa) case was also measured without the filter. The imaged shock diameter was found to be identical to the 150 psi (1.03 MPa) case with the filter (not shown), but was measurable over a wider viewing window. The shock diameter scales as $t^{-1/2}$. Because the total number of injected particles is linear in the valve opening time, i.e., $P_B \sim P_o t$, the diameter's time dependence is consistent with the expected $(P_o/P_B)^{1/2}$ scaling from [18]. While P_o does drop $\sim 10\%$ over the duration of the pulse, this only produces a small degree of systematic error in the fit, and it is clear from Figure 6 that this effect is negligible. The diameter ceases to shrink once the Mach disk moves into view, and appears to depend linearly on P_o ; the Mach disk diameter of the 50, 100, and 150 psi (0.35, 0.69, and 1.03 MPa) cases are 0.7, 1.5, and 2.2 cm, respectively.

4.4. Effects of Nozzle Design and Temperature on Jet Central Density

The detailed e-beam measurements enabled the optimization of the MCI system. To compare various nozzle conditions, the density along the jet axis (“central density”) is plotted in Figure 7. Operating the 4.5° injector at 80 K instead of 295 K increases the density by a factor of 6. This is a 60% larger increase than that predicted by the ideal gas law for a temperature change at fixed pressure. This implies that the cooling creates additional collimation in the flow, even for relatively modest backing pressures. For the 80 K injector with a backing pressure of 50 psi (0.35 MPa), switching from the 45° (Mach 3) nozzle to the 4.5° (Mach 5.5) design increased the central density by an order of magnitude. Operating at 295 K with the 45° nozzle produces jet densities below the sensitivity of the e-beam system, which is $\sim 1 \cdot 10^{15} \text{ cm}^{-3}$. This reinforces the importance of nozzle design, even for room-temperature injectors. Note also that

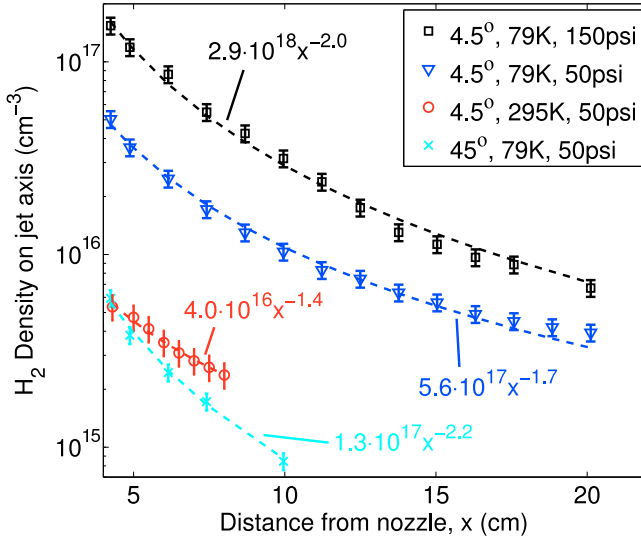


Figure 7. Replacing the 45° nozzle with the 4.5° nozzle raises the central density by an order of magnitude. Cooling the 4.5 nozzle from 295 K to 80 K increases the central density by a factor of 6. The density increases as the backing pressure is increased from 50 psi (0.35 MPa) to 150 psi (1.03 MPa). Each data set was fit with a power law, with the highest pressure case best fitting the predicted x^{-2} .

that increasing the backing pressure from 50 to 150 psi (0.35 to 1.03 MPa) increases the central density by a factor of ~ 3 , as expected.

The data from each set of conditions was fit with a power law of the form $n_{H_2} = ax^b$, where x is the distance from the nozzle. The expected value for a supersonic jet in vacuum is $b = -2$ [18]. The highest density data conforms extremely well to the x^{-2} dependence, but some of the lower density data deviates significantly. The 295 K injector, for example, does not produce a measurable shock structure. Its $x^{-1.4}$ dependence implies that background gas may be penetrating the jet interior and flattening the density gradient.

5. Measurement of Flow Rates and Comparison of Pressure Transducer Response to Electron Beam Measurements

Measurements of the jet produced by the injector with the 45° nozzle were taken with a 4 mm diameter Entran EPX pressure transducer (Measurement Specialties, Hampton, VA, USA). The apparatus is similar to that in Figure 3, but with the e-beam replaced by the pressure transducer on a movable vacuum feedthrough. The transducer membrane is aligned with the jet axis, and is moved between gas pulses to collect profiles of the response across the jet radius. The transducer measurements of the jet from the 80 K injector were dominated by a long time-scale response, from thermal deformation and relaxation of the membrane due to contact with the cold jet. This response was measured on the jet axis for 3 ms pulses at a variety of valve backing pressures. It was found to be proportional to the total number of injected particles, see Figure 8. Because the on-axis particle flux scales linearly with the particle throughput, the transducer response is a measure of the time-integrated particle flux

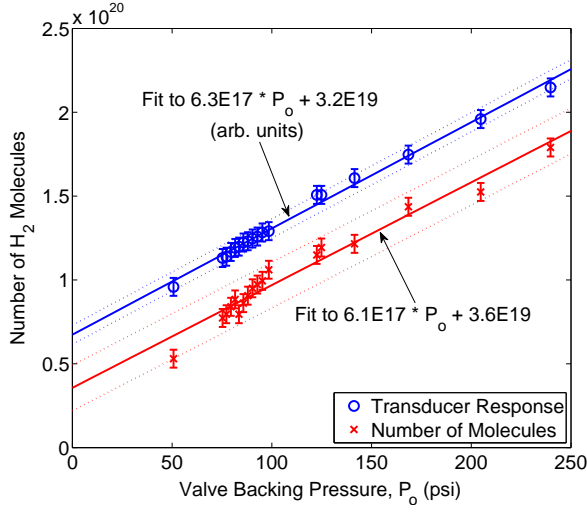


Figure 8. The transducer response and the number of H_2 molecules injected per pulse for a 3 ms opening are both described well with linear fits (shown with 90% confidence intervals). The full scale of 0-250 psi is equivalent to 0-1.75 MPa.

during a pulse.

The total particle injection rates in Figure 8 are $1.5 \cdot 10^{22} - 6 \cdot 10^{22}$ H_2 molecules/second for P_o of 50-250 psi (0.35-1.75 MPa). Because the valve is rated to operate up to 1250 psi (8.62 MPa), total fueling rates well over 10^{23} H_2 molecules/second should be possible. The 4.5° nozzle was confirmed to have the same throughput as the 45° nozzle; the flow rates in Figure 8 are applicable to both. The injection rate was also found to be linear in the valve opening time (not shown).

Figure 9 contains profiles of the transducer response from the 80 K injector with the 45° nozzle and a P_o of 50 psi (0.35 MPa). The transducer profiles were measured 3, 5, and 10 cm from the nozzle, and the density profiles obtained with the e-beam method have been overlaid in the latter two cases. The arbitrary transducer response has been normalized to the densities obtained with the e-beam. The transducer measurements confirm that the central density produced by the 45° nozzle falls off quickly from 3 to 10 cm, leaving a hollow profile (a low central density contained within the barrel shock). The estimated barrel shock radius is marked with a pair of arrows in each subplot, with the radius expanding away from the nozzle as expected. The qualitative agreement between the two methods validates the recently developed e-beam method.

6. Discussion on Cluster Formation and the Expected Cluster Population

The density profiles measured in this work are consistent with supersonic flows suitable for cluster formation. Similar nozzles operated at liquid nitrogen temperatures have been extensively studied and shown to produce cluster populations. We note that other than the density increase associated with improved collimation, there is not expected to be a large change in the flow close to the nozzle due to the cluster formation process [15]. Our results are consistent with this, as the cryogenic jets have the familiar shock

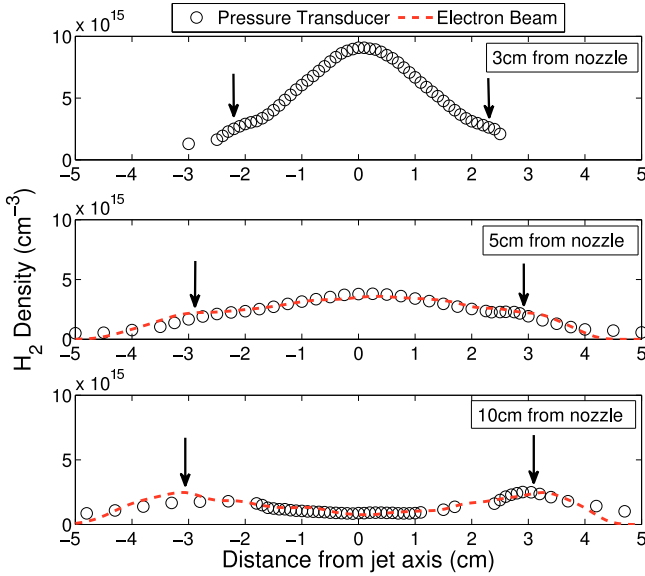


Figure 9. The pressure transducer response profiles and the e-beam profiles agree qualitatively. The estimated location of the barrel shock is noted by arrows.

structure of supersonic jets in vacuum. The zone of silence was measured to extend far from the nozzle (at least 20cm) for modest pulse lengths. Therefore free-streaming clusters and supersonic molecules should propagate to LTX plasmas with few collisions.

Isentropic flow calculations for the 4.5° nozzle with an 80 K reservoir indicate that the gas at the outlet reaches temperatures as low as 11 K, see Figure 10. For P_o of at least 100 psi (0.69 MPa), this is sufficient to reach the solid-gas vapor pressure curve [26]. Additional cooling is expected as the gas expands into vacuum. We do not suggest that cluster formation process in a pulsed nozzle is identical to an equilibrium phase change, merely that it is reasonable to expect substantial cluster formation under these conditions. Also of note in Figure 10 is that increasing the backing pressure monotonically increases the fraction of nozzle parameter space near the phase transition.

Precise determinations of cluster size and density depend on the details of the valve and nozzle construction, but we note that an empirical scaling law governing cluster formation exists, as defined by the Hagen parameter, Γ^* [24]:

$$\Gamma^* = k \frac{d^{0.85}}{T_o^{2.29}} P_o \quad (2)$$

with T_o the gas reservoir temperature in Kelvin, P_o the backing pressure in mbar, d the nozzle throat diameter in μm , and k a constant factor for each gas (184 for H_2). This formula is only valid for sonic nozzles. When using conical supersonic nozzles, a formula for the “equivalent nozzle diameter,” d_{eq} , is substituted in the place of d in equation 2 [27]:

$$d_{eq} = 0.866 \frac{d}{\tan \alpha} \quad (3)$$

Where the factor of 0.866 is for diatomic gases, α is the nozzle expansion half-angle, and d is the nozzle throat diameter in μm . The d_{eq} for the 45° and 4.5° nozzles

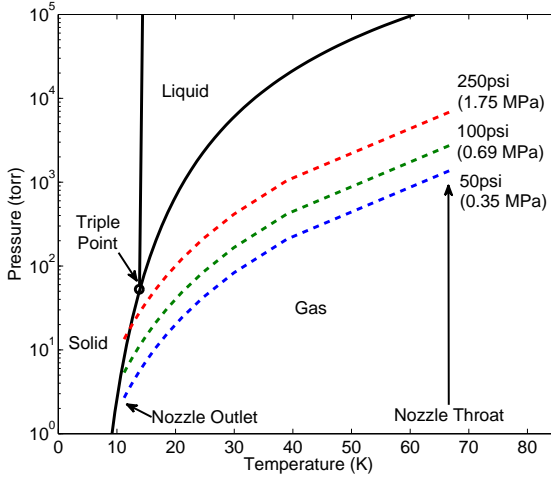


Figure 10. The phase diagram of H_2 , and the isentropic flow calculations for the 4.5° nozzle with backing pressures of 50, 100, and 250 psi (0.35, 0.69, and 1.75 MPa). Moving from right to left along the isentropes spans the parameters in the nozzle from throat to outlet. Because the nozzle outlet conditions reach the phase transition, cluster formation is expected.

used in this study are $440 \mu\text{m}$ and $5590 \mu\text{m}$, respectively, implying that for the same particle throughput, the 4.5° nozzle design yields an order of magnitude improvement in cluster formation.

Cluster formation begins for Γ^* of 100-300. The Mach 5.5 nozzle throat is $508 \mu\text{m}$, α is 4.5° , and P_o generally spans 50-250 psi (3500-17500 mbar). For this pressure range, at room-temperature (295 K), $\Gamma^* = 2200$ -11000, and at 80 K, $\Gamma^* = 4 \cdot 10^4$ - $2.2 \cdot 10^5$, suggesting a substantial increase in cluster formation when the nozzle is cooled. Earlier work on similar cluster fueling systems reported Γ^* about a factor of ten lower [6]. The primary reason for the higher Γ^* in this work is the design of the nozzle, i.e., the smaller α .

Following [13], the number of molecules per cluster, N , can be estimated, when $\Gamma^* < 10^4$:

$$N = 33 \left(\frac{\Gamma^*}{1000} \right)^{2.35} \quad (4)$$

and when $\Gamma^* > 10^4$:

$$N = 100 \left(\frac{\Gamma^*}{1000} \right)^{1.8} \quad (5)$$

For P_o of 50-250 psi (0.35-1.75 MPa) at 295 K, cluster sizes from 210-9200 H_2 molecules are expected. For the same P_o , but with the MCI cooled to 80K, cluster sizes of $9 \cdot 10^4$ - $1.7 \cdot 10^6$ molecules are expected.

The ionization cross-section of clusters is known to be reduced relative to an equal number of gas-phase molecules, thought to be from a shielding of inner molecules by the outer molecules in a cluster [7]. This reduction is negligible for clusters of less than 10^4 molecules, and scales with the cluster size, as $N^{-2/3}$. For example, clusters

of $\sim 10^5$ molecules have an equivalent ionization cross-section that is about 30% less than that of a single H_2 molecule. It may be possible to exploit this cross-section reduction in a fueling system to improve the depth of fueling into a plasma. Because the clusters are a minority population, maximizing the cluster population and limiting the gas throughput to the plasma may be necessary to achieve significant improvement. In reference [13], with a nearly identical nozzle geometry and Γ^* comparable to the 250 psi (1.75 MPa) jets in this work, the fraction of molecules contained in a cluster (the condensation fraction) close to the nozzle outlet was estimated to be about 20%. Possible ways of maximizing the large cluster fraction and other similar considerations are discussed in section 7.

It should be noted that the effect of the ionization cross-section reduction on the e-beam measurements presented in this work is expected to be small. The quantitative density measurements in this work were limited to P_o of 150 psi (1.03 MPa) or less. For a condensation fractions under 20%, this implies a less than $\sim 5\%$ reduction in the population-averaged ionization cross-section, with a roughly equal underestimate of the molecular density determined from the H_α emission. This is well within the existing error of the e-beam method. Furthermore, because the jet is highly directed, the relative fraction of gas-phase and cluster-phase molecules does not vary strongly away from the nozzle, and reaches an asymptotic value in the zone of silence [23], making the error roughly constant across the region of interest. Thus the measurements presented here should be an accurate representation of the molecular densities produced by the MCI.

7. Implications for Fueling Performance on the LTX

The MCI produces a collimated particle source suitable for testing short-pulse, high-density fueling on the LTX. Molecular densities in excess of 10^{15} cm^{-3} exist more than 20 cm from the nozzle. The LTX electron densities are 10^{12} - 10^{13} cm^{-3} , so $n_{H_2} = 100 - 1000 n_e$. Electron temperatures are expected to be at most a few hundred eV in the plasma core. Because the e-beam used for the measurements in this work has an energy of 250 eV, it can be used to approximately predict how LTX electrons will interact with MCI fueling. Depending on the value of P_o , and therefore the resulting neutral density, the mean-free-path of 250 eV electrons can be either comparable to or significantly smaller than the supersonic jet size, resulting in negligible, partial, or complete e-beam attenuation. The percentage of the e-beam that is absorbed, Λ , is determined from the drop in the H_α intensity, I , across the jet, measured at two points equidistant from the jet center:

$$\Lambda = \frac{I_{initial} - I_{final}}{I_{initial}}. \quad (6)$$

Figure 11 contains the percentage of attenuation across various cryogenic (80 K) MCI jets. Λ approaching 100% can be obtained 5 cm from the nozzle with P_o in excess of 150 psi (1.03 MPa), and 10 cm from the nozzle with P_o of 250 psi (1.75 MPa). The attenuation fraction falls as the distance from the nozzle is increased, but reaches an asymptotic value as the jet parameters cease to vary strongly. Because the temperatures in early LTX experiments are expected to be less than 250 eV, the measurements in Figure 11 provide a lower-bound on the ability of an MCI fueling pulse to fully absorb LTX electrons.

The main implication of Figure 11 is that by varying P_o and the location of the MCI nozzle relative to the plasma edge, the MCI can be used to explore distinct

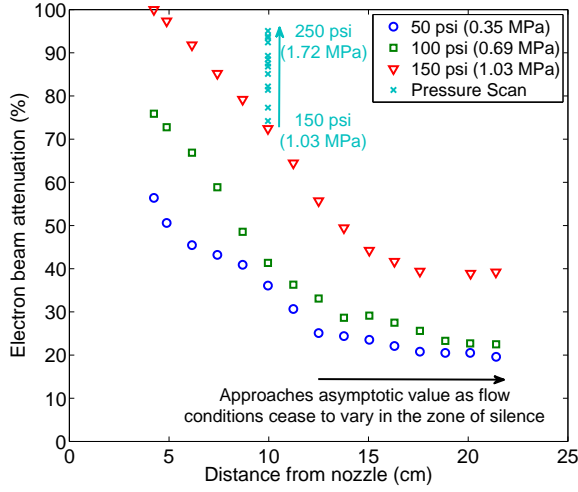


Figure 11. The degree of e-beam attenuation across the jet width, determined by the reduction in H_{α} emission. The variation along the jet axis for three discrete pressures follows a similar functional form, and a pressure scan demonstrates that it is possible to deplete the 250 eV e-beam 10 cm from the nozzle for P_o approaching 250 psi (1.75 MPa). This implies that it will be possible to study the physics of highly dense fueling on the LTX.

fueling regimes. For relatively low Λ , the physics is expected to be similar to that of a conventional gas puffer, where the depth of fueling is determined by the mean-free-path of individual molecules. At high Λ , it is expected that significant “pellet-like” collective effects will manifest, i.e., inner molecules in the jet will be shielded by outer molecules, allowing them to penetrate deeper into the plasma.

Furthermore, the presence of very large clusters in the flow provides another possible means for increasing the depth of fueling, through the reduction of the ionization cross-section. While it is true that for the MCI parameters discussed here, the fraction of clusters in the flow is not expected to exceed 20-25%, there may be a preferential deposition of large clusters deeper in the plasma, while individual molecules and small clusters are ionized closer to the plasma edge. The relative importance of the cluster size and high molecular density for enhancing the depth of fueling is currently unknown, and we expect experiments on the LTX will elucidate on this point.

Experiments on HL-2A indicated molecular cluster fueling depths exceeding those from gas puffers and room-temperature supersonic gas jets, while pellet injection produced even deeper fueling [6]. This is consistent with the concept of clusters as very small pellets. LTX is a smaller machine, with a minor radius of 26cm, versus 40cm on HL-2A. Because HL-2A measured fueling depths of 25-32 cm at similar n_e with the cluster injection system, it is anticipated that cluster injection will be sufficient to provide a high fraction of core fueling on the LTX. To maximize the depth of fueling, Figure 11 and equations 2, 4, and 5 imply the highest possible P_o should be used, producing the largest clusters and the highest total molecular densities.

However, this could produce total particle injection rates that exceed the fueling requirements of LTX plasmas. For present operations LTX has a particle inventory

of $\sim 10^{19}$ particles. For the projected future operation at ~ 200 kA, the Greenwald density limit is $\sim 10^{20} \text{ m}^{-3}$, or about $1.2 \cdot 10^{20}$ particles [28]. Figure 8 implies that even for backing pressures below 100 psi (0.69 MPa), the MCI can replace the entire plasma particle inventory with a 3 ms pulse. One possible solution is to place a skimmer in the zone of silence, allowing only the supersonic molecules and clusters in the center of the jet to pass into the plasma. The subsonic gas outside of the barrel shock is excluded, limiting the total particle throughput and maximizing the relative fraction of clusters in the flow. Furthermore, because clusters inherit the average trajectory of their constituent molecules, the largest clusters are expected to concentrate on-axis, and a skimmer on the jet axis will tend to collect the largest clusters from the flow.

Skimmers are routinely used for cluster accelerator targets [29, 30]. Noting Figures 5 and 6, it is clear that the skimmer should be no larger than 4 cm in diameter to exclude the barrel shock. It should also be located upstream of the Mach disk, but cannot be too close to the nozzle or an attached shock at the skimmer edge may disrupt the flow. Thus the skimmer designed for the MCI has a diameter of 2.5 cm, and is located 5-10 cm from the nozzle. To mitigate the build-up of P_B upstream of the skimmer, a 2000 liter/second SAES getter pump (SAES Getters, Lainate, Italy) has been installed.

With the addition of a skimmer, it is possible to independently test the relative contributions of the cluster population and the high molecular density. Skimmed flows will have a relatively high fraction of molecules located in clusters. However, with the high-density barrel shock region removed, they will produce less shielding of neutrals in the interior of the flow, i.e., a lower Λ . If these flows produce deeper fueling than room-temperature supersonic gas injection, this will confirm that the reduction of the cluster ionization cross-section can produce deeper fueling. Alternatively, if they behave similarly to room-temperature supersonic jets of comparable density, this will indicate that the cluster population is only useful as a means to produce collimated, high-density flows. In the latter case, it may be more fruitful to pursue nozzle designs that maximize the molecular density at the expense of efficient cluster formation. Successful optimization of the fueling penetration on LTX is expected to motivate installation of similar systems on other machines, providing deeper fueling and better control of the particle source than gas-puffers, and as a less technically complex alternative to pellet injection systems.

8. Conclusions

A high-density fueling system has been developed for the LTX experiment, with total fueling rates measured at $1.5 \cdot 10^{22} - 6 \cdot 10^{22} \text{ H}_2$ molecules/second. Detailed electron-beam fluorescence measurements indicate molecular densities well over 10^{15} cm^{-3} far from the nozzle, which are suitable for high-density fueling of LTX plasmas. Complementary measurements with a pressure transducer are found to have good qualitative agreement, validating the e-beam results. The nozzle design was improved, yielding an order of magnitude increase in the jet central density. Cryogenic cooling was also found to substantially increase the molecular density in the flow, demonstrating an improvement over conventional (room-temperature) supersonic gas injectors. The diameter of the supersonic jet structure was measured with 250 μs resolution, and found to scale as $(P_o/P_B)^{1/2}$, consistent with earlier studies of supersonic flows in vacuum. The measured density profiles and shock structures are consistent with supersonic flow conditions suitable for the creation of molecular

clusters. This provides confidence in using previously derived empirical scaling laws to predict the properties of the cluster population. It was demonstrated that the supersonic jets created by the MCI can fully absorb 250 eV electrons, suggesting that the depth of fueling on the LTX should exceed that of lower density gas fueling systems.

Acknowledgments

This work was supported by U.S. Department of Energy Contract Number DE-AC02-09CH11466.

References

- [1] Baylor L, Jernigan TC, Colchin RJ, Jackson GL, Owen LW and Petrie TW. 2003 *J. Nucl. Mater.* **313-316** 530-533
- [2] Pegourie B *et al.* 2003 *J. Nucl. Mater.* **313-316** 539-542
- [3] Soukhanovskii VA, Kugel HW, Kaita R, Majeski R and Roquemore AL. 2004. *Rev. Sci. Instrum.* **75** 4320-4323
- [4] Gray T, Kaita R, Majeski R, Spaleta J and Timberlake J. 2006. *Rev. Sci. Instrum.* **77** 10E901
- [5] Klingelhofer R and Moser HO. 1972. *J. App. Phys.* **43** 4575-4579
- [6] Yao L *et al.* 2007. *Nucl. Fusion.* **47** 1399-1410
- [7] Henkes W and Mikosch F. 1974. *Int. J. Mass Spectrom. Ion Phys.* **13** 151-161
- [8] Jiao Y, Zhou Y, Yao L, and Dong J. 2003. *Plasma Phys. Control. Fusion.* **45** 2001-2010
- [9] Majeski R *et al.* 2009. *Nucl. Fusion.* **49** 055014
- [10] Majeski R *et al.* 2006 *Phys. Rev. Lett.* **97** 075002
- [11] Krasheninnikov SI, Zakharov LE, and Pereverzev GV. 2003. *Phys. Plasmas.* **10** 1678.
- [12] Majeski R *et al.* 2009 *Nucl. Fusion.* **49** 055014
- [13] Dorchie F, Blasco F, Caillaud T, Stevefelt J, Stenz C, Boldarev AS and Gasilov VA. 2003. *Phys. Rev. A.* **68** 023201
- [14] Smith RA, Ditmire T and Tisch JWG. 1998. *Rev. Sci. Instrum.* **69** 3798-3804
- [15] Bickel W, Buschmann M, Dombroski H, Gaul G, Grzonka D, Holker G, Santo R and Wahning M. 1990. *Nucl. Instrum. Methods A.* **295** 44-52
- [16] Khoukaz A, Lister T, Quentmeier C, Santo R and Thomas C. 1999. *Eur. Phys. J. D.* **5** 275-281
- [17] Campargue R. 1984. *J. Phys. Chem.* **88** 4466-4474
- [18] Ashkenas H and Sherman FS. 1966. *Rarefied Gas Dynamics* **2** (New York: Academic) 84-105
- [19] Be SH, Yano K, Enjoji H and Okamoto K. 1975. *Jpn. J. Appl. Phys.* **14** 1049
- [20] Gochberg LA. 1997. *Prog. Aerosp. Sci.* **33** 431
- [21] Janev RK, Langer WD, Evans K and Post DE. 1987. *Elementary Processes in Hydrogen-Helium Plasmas*, Springer
- [22] Lundberg DP, Kaita R, Majeski R and Stotler DP. 2010 *Rev. Sci. Instrum.* 10D707
- [23] Khmel SY and Sharafutdinov RG. 1997. *Tech. Phys.* **42** 986
- [24] Hagena OF. 1987. *Z. Phys. D.* **4** 291
- [25] Hagena OF. 1992. *Rev. Sci. Instrum.* **63** 4
- [26] Souers PC. 1979. *Cryogenic Hydrogen Data Pertinent to Magnetic Fusion Energy*. UCRL05268, LLNL
- [27] . Hagena OF. 1981. *Surf. Sci.* **106** 101
- [28] Greenwald M 2002. *Plasma Phys. Control. Fusion* **44** R27-R80
- [29] Reich H, Bourgeois W, Franzke B, Kritzer A and Varentsov V. 1997. *Nucl. Phys. A.* bf 626 417c-425c
- [30] Kramer A, Kritzer A, Reich H and Stohlker Th. 2001. *Nucl. Instrum. Meth. B.* **174** 205-211

The Princeton Plasma Physics Laboratory is operated
by Princeton University under contract
with the U.S. Department of Energy.

Information Services
Princeton Plasma Physics Laboratory
P.O. Box 451
Princeton, NJ 08543

Phone: 609-243-2245
Fax: 609-243-2751
e-mail: pppl_info@pppl.gov
Internet Address: <http://www.pppl.gov>